Recent results on e^+e^- annihilation to hadrons in the SND experiment

M. N. Achasov^{a,b}, A. Yu. Barnyakov^{a,c}, A. A. Baykov^{a,b}, K. I. Beloborodov^{a,b}, A. V. Berdyugin^{a,b}, A. G. Bogdanchikov^a,
A. A. Botov^a, T. V. Dimova^{a,b}, V. P. Druzhinin^{a,b}, V. B. Golubev^a, L. V. Kardapoltsev^{a,b}, A. G. Kharlamov^{a,b},
A. A. Korol^{a,b}, D. P. Kovrizhin^a, A. S. Kupich^{a,b}, K. A. Martin^a, N. A. Melnikova^a, N. Yu. Muchnoy^{a,b}, A. E. Obrazovsky^a,
E. V. Pakhtusova^a, K. V. Pugachev^{a,b}, Ya. S. Savchenko^{a,b}, S. I. Serednyakov^{a,b}, D. A. Shtol^a, Z. K. Silagadze^{a,b},
I. K. Surin^a, Yu. A. Tikhonov^{a,b}, Yu. V. Usov^a, V. N. Zhabin^{a,b}, V. V. Zhulanov^{a,b} (SND Collaboration)

^{a}*Budker Institute of Nuclear Physics, Novosibirsk, 630090, Russia.*
^{b}*Novosibirsk State University, Novosibirsk, 630090, Russia.*
^{c}*Novosibirsk State Technical University, Novosibirsk, 630092, Russia.*

Recent results of the SND experiment at the VEPP-2000 collider on e^+e^- annihilation to hadrons below 2 GeV are presented. In particular, we discuss measurements of the $e^+e^- \to \pi^+\pi^-$ and $e^+e^- \to n\bar{n}$ cross sections. The processes $e^+e^- \to \pi^+\pi^-\pi^0$, $K^+K^-\pi^0$, $\eta\pi^0\gamma$ and $2\eta\gamma$ were under investigation as well. The preliminary results on the $e^+e^- \to \omega\pi^0 \to \pi^+\pi^-2\pi^0$ cross section measurement are also presented.

1. Introduction

VEPP-2000 is an electron-positron collider with the center-of-mass energy from 0.3 to 2 GeV located at Budker Institute of Nuclear Physics in Novosibirsk, Russia [1]. The collider has a circumference of about 24 m and utilizes the concept of round beams. The achieved luminosity is 4×10^{-31} cm^{-2}s^{-1}. Two multi-purpose particle detectors, SND and CMD-3, are installed at the opposite points of the VEPP-2000 collider.

SND, Spherical Neutral Detector, is a multi-purpose non-magnetic detector. It has two main systems: spherical NaI electromagnetic calorimeter and non-magnetic multi-wire drift chamber, which are used for measuring particles' angles and energies. The auxiliary components, muon veto system, comprised of proportional tubes and scintillator counters, and aerogel threshold Cherenkov counters, are used for particle identification.

The experiments with SND at VEPP-2000 started in 2010. During the period from 2013 to 2016 the collider was upgraded to achieve higher luminosity. In eight years of its operation the detector has collected 370 pb^{-1} of integrated luminosity, including more than 260 pb^{-1} at energies above the ϕ meson resonance. Significant portions of data were collected in the energy ranges of the ρ, ω and ϕ mesons, as well as of the f_1 meson and $n\bar{n}$ threshold.

2. Analysis

2.1. Process $e^+e^- \to \pi^+\pi^-$

One of the recent SND results is the measurement of the $e^+e^- \to \pi^+\pi^-$ process cross section [2] (Fig. 1). The analysis is based on the statistics collected below 980 MeV in
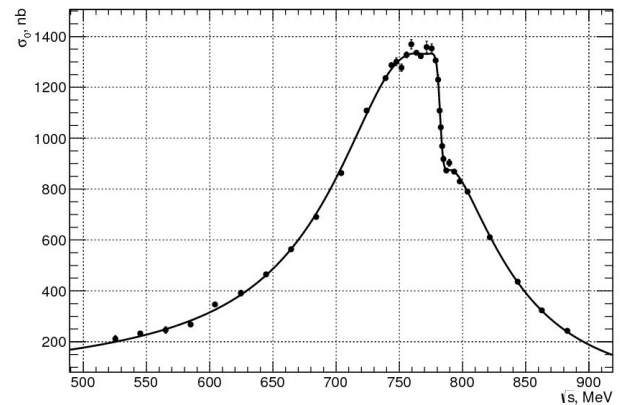

FIGURE 1. The Born cross section of the $e^+e^- \to \pi^+\pi^-$ process [2].

center-of-mass in 2013. The background $e^+e^- \to e^+e^-$ events were separated from $\mu^+\mu^-$ and $\pi^+\pi^-$ events using machine learning [3]. The BDT classification is based on differences in calorimeter energy depositions, which is the result of differences in electromagnetic shower shapes. The $\mu^+\mu^-$ events were subtracted from the selected events, where the number was taken from QED prediction. The remaining events were taken to be signal events of the $e^+e^- \to \pi^+\pi^-$ process. The contribution of trigger to systematic uncertainty is 0.5 %, selection criteria give 0.6 %, and particle identification gives up to 0.5 %. The uncertainty of nuclear interaction simulation and theoretical prediction give 0.2 % each, resulting in a total systematic uncertainty below 1.0 %. The measured cross section was fitted with the vector-meson dominance model to obtain the Born cross section and the parameters of the ρ meson. The obtained values of the parameters were found to be in agreement with PDG values. The obtained cross section is in agreement with VEPP-2M measure-
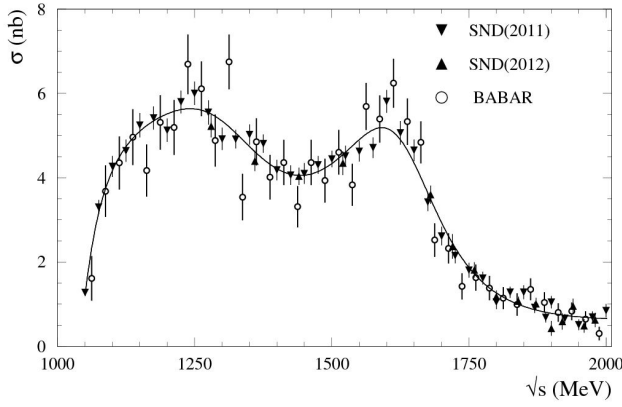
FIGURE 2. The Born cross section of the $e^+e^- \rightarrow \pi^+\pi^-\pi^0$ process [7–9]. The model for the fitting line takes into account the contributions of the $\omega(782)$, $\phi(1020)$, $\omega(1420)$ and $\omega(1650)$ resonances. The latter two correspond to two peaks visible in the cross section.

ments [4], but there is a slight discrepancy with BaBar [5] and KLOE [6] measurements. The contribution to the anomalous magnetic moment of the muon a_μ from the $\pi^+\pi^-$ intermediate state was calculated to be $(409.79 \pm 1.44 \pm 3.87) \times 10^{-10}$ (the first error is statistical, the second is systematical).

2.2. Process $e^+e^- \rightarrow \pi^+\pi^-\pi^0$

Another recent SND result in the analysis of the $\pi^+\pi^-\pi^0$ dynamics in the energy range 1–2 GeV [7]. The cross section of this process was also measured (Fig. 2), with the systematic uncertainty less than 5 %, and agrees with previous SND and BABAR measurements [8, 9]. The events of the signal process were selected by requiring two tracks from charged pions and two photons with energies above 30 MeV. Collinear background processes were rejected by the condition imposed on azimuthal angles of tracks. In order to investigate the dynamics of the $\pi^+\pi^-\pi^0$ process, we fitted the two-dimensional distributions of the charged-pion momenta (Dalitz plot) and the invariant mass destribution for the $\pi^+\pi^-$ pair. The model used in the fitting procedure is the sum of the $\rho\pi$ and $\omega\pi^0$ intermediate states, where ρ is either the $\rho(770)$ or $\rho(1450)$ state. The amplitude of the $\omega\pi^0$ mechanism was fixed from the $e^+e^- \rightarrow \omega\pi^0 \rightarrow 2\pi^0\gamma$ cross section [10]. The energy range with significant contribution of the radiative process $e^+e^- \rightarrow \phi\gamma$ (1.05–1.15 GeV) was omitted from the analysis. The contribution of the $\rho(1450)\pi$ intermediate state is observed near the energy of the $\omega(1650)$ resonance. At our level of statistics we cannot separate the $\rho(1700)$ from the $\rho(1450)$ contribution. We conclude that the decay $\omega(1650) \rightarrow \pi^+\pi^-\pi^0$ is mediated by the $\rho(1450)$ state and the decay $\omega(1420) \rightarrow \pi^+\pi^-\pi^0$ in turn is mediated by the $\rho(770)$ state.

2.3. Process $e^+e^- \rightarrow K^+K^-\pi^0$

The analysis of the process $e^+e^- \rightarrow K^+K^-\pi^0$ is based on 26 pb^{-1} of data in the energy range from 1.2 to 2.0 GeV
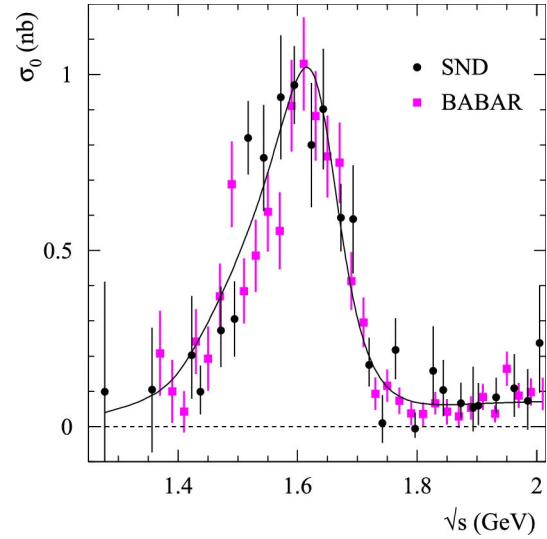

FIGURE 3. The born cross section of the $e^+e^- \rightarrow K^*K \rightarrow K^+K^-\pi^0$ process [11, 12].

[11]. The cross sections of the two main intermediate states of this process, $K^*(892)K$ (Fig. 3) and $\phi\pi^0$ (Fig. 4), were measured separately. The mass spectrum of the $K^\pm\pi^0$ system indicates that the process $e^+e^- \rightarrow K^+K^-\pi^0$ is dominated by the K^*K intermediate state, while $\phi\pi^0$ gives only much smaller contribution. The interference between these mechanisms was found to give a significant contribution to the $e^+e^- \rightarrow \phi\pi^0 \rightarrow K^+K^-\pi^0$ cross section resulting in the systematical uncertainty reaching 30 %. Also we found that the $K^*(892)K$ mechanism is dominated by the $\phi(1680)$ state.

The SND results are consistent with the measurements in the BABAR [12, 13] experiment and have comparable accuracy. The contribution of an unknown resonance with the mass near 1.6 GeV is required in addition to ρ mesons to
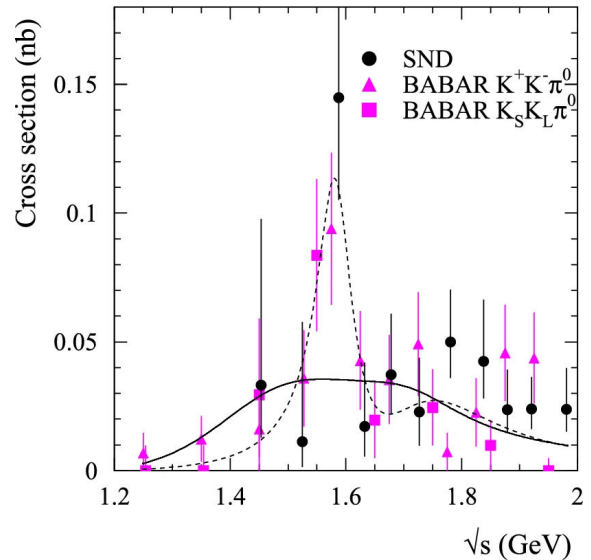

FIGURE 4. The Born cross section of the $e^+e^- \rightarrow \phi\pi^0 \rightarrow K^+K^-\pi^0$ process [11–13].
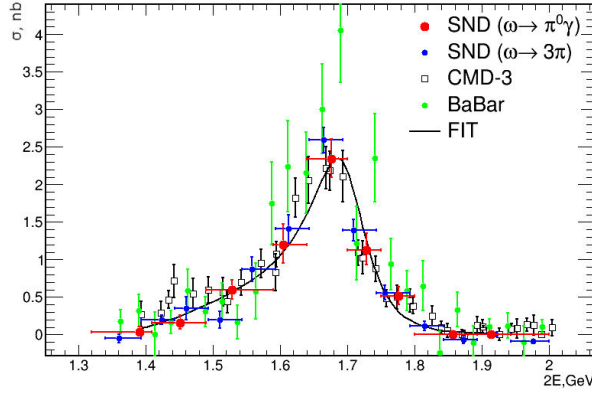
FIGURE 5. The Born cross section of the $e^+e^- \to \omega\eta \to \eta\pi^0\gamma$ process [14–17].

FIGURE 6. The Born cross section of the $e^+e^- \to \eta\eta\gamma$ process [21] in comparison with the expected value from the $e^+e^- \to \phi\pi^0$ cross section measurement [19].

describe the cross section of the $\phi\pi^0$ mechanism. Its significance calculated from the difference of the χ^2 values for the model with the $\rho(1700)$ resonance and a resonance with free parameters and the model with the $\rho(1450)$ and $\rho(1700)$ states is about 3σ. This anomaly is present in both SND and BABAR measurements.

2.4. Process $e^+e^- \to \eta\pi^0\gamma$

The process $e^+e^- \to \eta\pi^0\gamma$ is studied in the energy range 1–2 GeV for the first time [14]. The analysis uses more than 100 pb^{-1} of data in five-photon final state. The fit to the $\pi^0\gamma$ invariant-mass distribution was used for the study of intermediate states. The main intermediate state of the process was found to be $\omega\eta$. Its cross section is in agreement with measurements in the $\omega \to \pi^+\pi^-\pi^0$ decay channel (Fig. 5) made in SND, CMD-3 and BABAR experiments [15–17]. We found that the contribution of other hadronic mechanisms $\rho\eta$, $\phi\eta$, $\phi\pi^0$, $\omega\pi^0$ and $\rho\pi^0$, calculated from existing measurements [10,12,13,18,19], is insufficient to describe the rest of the $e^+e^- \to \eta\pi^0\gamma$ process after subtracting the $\omega\eta$ component. Thus we expect that there is a contribution of radiative processes, such as $a_0(980)\gamma$, $a_0(1450)\gamma$ and $a_2(1320)\gamma$, at the level of about 15–20 pb in a wide energy range. The shape of the $\eta\pi^0$ invariant mass spectrum suggests that $a_0(1450)\gamma$ is the main mechanism of this radiative process. The theoretical prediction based on the framework of the quark model [20] gives the radiative part of the cross section about 3–5 pb which is much smaller than our measurement.

2.5. Process $e^+e^- \to 2\eta\gamma$

The cross section of $e^+e^- \to 2\eta\gamma$ is measured in the energy range 1–2 GeV for the first time (Fig. 6) [21]. The number of $\eta\eta\gamma$ events is determined by fitting the distribution of difference $\chi^2_{\eta\eta\gamma} - \chi^2_{5\gamma}$ of χ^2-values of kinematic reconstruction in two hypotheses for the selected events. Based on the cross section of the processes $e^+e^- \to \phi\pi^0 \to K^+K^-\pi^0$, $e^+e^- \to \omega\eta \to \pi^+\pi^-\pi^0\eta$ and $e^+e^- \to \rho\eta \to \pi^+\pi^-\eta$ measured in [15, 18, 19], we expect the $\phi\eta$ to be the main intermediate state. This expectation is confirmed by the fact

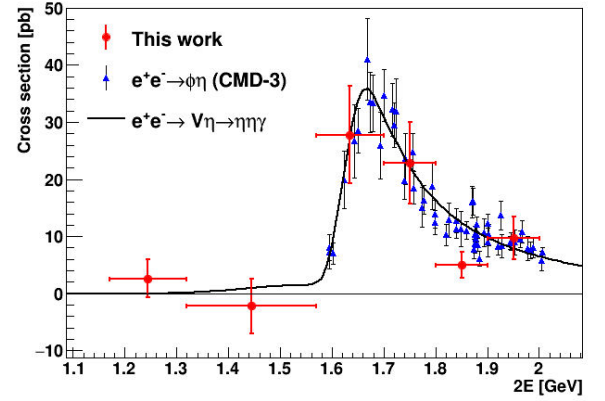that the measured cross section is consistent with the CMD-3 result made with decay of $\phi \to K^+K^-$ [19]. The contribution from intermediate states other than $V\eta$ (V stands for a vector meson), such as radiative processes $f_0(1500)\gamma$ and $f_2'(1525)\gamma$, is not observed even when the contribution of the main mechanism $\phi\eta$ is suppressed by kinematic constraints. Thus the upper limits on the radiative intermediate states, $f_0(1500)\gamma$ and $f_2'(1525)\gamma$, have been set using the CL_s technique [22, 23]. Their cross sections do not exceed 35 and 18 pb, respectively, below 1.8 GeV with 90 % CL.

2.6. Process $e^+e^- \to n\bar{n}$

The process of $n\bar{n}$ production is studied near its threshold. The analysis is based on 70 pb^{-1} of data collected by the SND detector. Events are selected using event time measurement in the EM calorimeter [24]. Before the calorimeter electronics upgrade in summer of 2017, the calorimeter trigger time was used. After the upgrade, the time was measured with flash ADC for each calorimeter channel, providing significantly better time resolution. The cross section is measured in the energy range from nucleon-antinucleon threshold up to 2 GeV. The measured value is about 0.4 nb and is slightly lower than previous measurements [25] but has significantly better accuracy.

The $n\bar{n}$ form factor consists of electric and magnetic contributions which have different dependence on polar angle θ. The fit of the $\cos\theta$ distributions was used to extract the ratio of G_E to G_M for different center of mass energies from the process threshold up to 2 GeV. At the current level of statistics the measured ratio of neutron form factors below 2 GeV agrees with unity.

2.7. Process $e^+e^- \to \omega\pi^0$

The analysis of $e^+e^- \to \omega\pi^0 \to \pi^+\pi^-2\pi^0$ is based on 35 pb^{-1} of data in the energy range 1–2 GeV, recorded by the SND detector in 2011 and 2012. We performed a kinematic fit to the $\pi^+\pi^-2\pi^0$ hypothesis and take events with $\chi^2 < 40$ for further analysis. The extraction of the $\omega\pi^0$ contribution
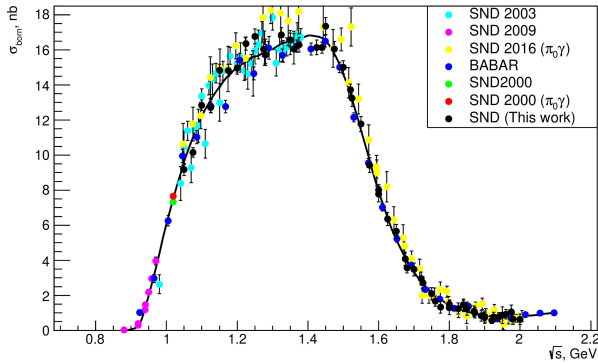
FIGURE 7. The Born cross section of the $e^+e^- \rightarrow \omega\pi^0 \rightarrow \pi^+\pi^-2\pi^0$ process [10, 26–29].

uses fitting of the $\pi^+\pi^-\pi^0$ invariant-mass spectrum. The number of $\omega\pi^0$ events, as well as of three other mechanisms of $e^+e^- \rightarrow \pi^+\pi^-2\pi^0$, $a_1\pi$, $\rho^+\rho^-$ and $f_0(980)\rho$, are free parameters of the fit, while the number of other background events is fixed from existing measurements.

The radiative correction and the Born cross section were obtained by fitting the measured $\omega\pi^0$ cross section (Fig. 7) with the vector-meson dominance model including three states from the ρ family. The comparison with the $\omega\pi^0 \rightarrow 2\pi^0\gamma$ cross section takes into account the phase space factor difference for ω decay channels. The cross section was obtained by limiting ω invariant mass below 0.9 GeV. This definition of the $\omega\pi^0$ cross section is expected to be independent of model for the ω resonance line shape. It is worth noting that the form factor $\gamma^*\omega\pi^0$ depends neither on the cross section definition nor on the ω line shape.

The systematic uncertainty of the cross section measurement is less than 5 % below 1.6 GeV and rises up to 16 % at 2 GeV. The measured cross section is in agreement with the previous measurements made at SND, CMD-3 and BABAR [10, 26–29].

3. Summary

The SND detector collected about 370 pb^{-1} of data since 2010 in the energy range from 0.3 to 2 GeV. The process $K^+K^-\pi^0$ was studied and its two intermediate states were separated. Rare radiative processes $\eta\pi^0\gamma$ and $2\eta\gamma$ have been studied. The new event time measurement method has significantly improved the accuracy of the $n\bar{n}$ cross section measurement. The dynamics of the $\pi^+\pi^-\pi^0$ process has been studied above 1 GeV. The $\omega\pi^0 \rightarrow \pi^+\pi^-2\pi^0$ cross section is measured with high precision and is in agreement with the previous measurements. The $\pi^+\pi^-$ cross section has been measured by SND with systematic uncertainty better than 1 % using machine learning.

1. P. Y. Shatunov *et al.*, Status and perspectives of the VEPP-2000, Phys. Part. Nucl. Lett. **13** (2016), 995, https://doi.org/10.1134/S154747711607044X.

2. M. N. Achasov *et al.* (SND collaboration), Measurement of the $e^+e^- \rightarrow \pi^+\pi^-$ process cross section with the SND detector at the VEPP-2000 collider in the energy region $0.525 < \sqrt{s} < 0.883$ GeV. J. High Energ. Phys. **2021** (2021), 113, https://doi.org/10.1007/JHEP01(2021)113.

3. M. N. Achasov, A. S. Kupich, Separation of electrons and pions in the SND detector calorimeter, Phys. Part. Nucl. **49** (2018), 64, https://doi.org/10.1134/S1063779618010021.

4. M. N. Achasov *et al.*, Update of the $e^+e^- \rightarrow \pi^+\pi^-$ cross section measured by the spherical neutral detector in the energy region $400 < \sqrt{s} < 1000$ MeV, J. Exp. Theor. Phys. **103** (2006), 380, https://doi.org/10.1134/S106377610609007X.

5. J. P. Lees *et al.* (BaBar collaboration), Precise Measurement of the $e^+e^- \rightarrow \pi^+\pi^-(\gamma)$ Cross Section with the Initial State Radiation Method at BABAR Phys. Rev. Lett. **103** (2009), 231801, https://doi.org/10.1103/PhysRevLett.103.231801.

6. A. Anastasi *et al.* (The KLOE-2 collaboration), Combination of KLOE $\sigma(e^+e^- \rightarrow \pi^+\pi^-(\gamma))$ measurements and determination of $a_\mu^{\pi^+\pi^-}$ in the energy range $0.10 < s < 0.95$ GeV^2, J. High Energ. Phys. **2018** (2018), 173, https://doi.org/10.1007/JHEP03(2018)173.

7. M. N. Achasov *et al.* (SND collaboration), Study of dynamics of the process $e^+e^- \rightarrow \pi^+\pi^-\pi^0$ in the energy range 1.15-2.00 GeV, Eur. Phys. J. C **80** (2020), 993, https://doi.org/10.1140/epjc/s10052-020-08524-4.

8. V. M. Aul'chenko *et al.*, Study of the $e^+e^- \rightarrow \pi^+\pi^-\pi^0$ process in the energy range 1.05-2.00 GeV, J. Exp. Theor. Phys. **121** (2015) 27, https://doi.org/10.1134/S1063776115060023.

9. B. Aubert *et al.*, Study of the $e^+e^- \rightarrow \pi^+\pi^-\pi^0$ process using initial state radiation with BABAR, Phys. Rev. D **70** (2004), 072004, https://doi.org/10.1103/PhysRevD.70.072004.

10. M. N. Achasov *et al.*, Updated measurement of $e^+e^- \rightarrow \omega\pi^0 \rightarrow \pi^0\pi^0\gamma$ cross section with the SND detector, Phys. Rev. D **94** (2016), 112001, https://doi.org/10.1103/PhysRevD.94.112001.

11. M. N. Achasov *et al.* (The SND collaboration), Measurement of the $e^+e^- \rightarrow K^+K^-\pi^0$ cross section with the SND detector Eur. Phys. J. C **80** (2020), 1139, https://doi.org/10.1140/epjc/s10052-020-08719-9.

12. B. Aubert *et al.*, Measurements of $e^+e^- \rightarrow K^+K^-\eta$, $K^+K^-\pi^0$, and $K_s^0 K^\pm\pi^\mp$ cross sections using initial state radiation events, Phys. Rev. D **77** (2008), 092002, https://doi.org/10.1103/PhysRevD.77.092002.

13. J. P. Lees *et al.* (BABAR Collaboration), Cross sections for the reactions $e^+e^- \rightarrow K_s^0 K_L^0 \pi^0$, $K_s^0 K_L^0 \eta$, and $K_s^0 K_L^0 \pi^0 \pi^0$

from events with initial-state radiation, Phys. Rev. D **95** (2017), 052001, https://doi.org/10.1103/PhysRevD.95.052001.

14. M. N. Achasov *et al.* (SND collaboration), Study of the process $e^+e^- \rightarrow \eta\pi^0\gamma$ in the energy range $\sqrt{s} = 1.05 - 2.00$ GeV with the SND detector, Eur. Phys. J. C **80** (2020), 1008, https://doi.org/10.1140/epjc/s10052-020-08556-w.

15. M. N. Achasov *et al.*, Measurement of the $e^+e^- \rightarrow \pi^+\pi^-\pi^0\eta$ cross section below $\sqrt{s} = 2$ GeV, Phys. Rev. D **99** (2019), 112004, https://doi.org/10.1103/PhysRevD.99.112004.

16. R. R. Akhmetshin *et al.*, Study of the process $e^+e^- \rightarrow \pi^+\pi^-\pi^0\eta$ in the c.m. energy range 1394-2005 MeV with the CMD-3 detector, Phys. Lett. B **773** (2017), 150, https://doi.org/10.1016/j.physletb.2017.08.019.

17. B. Aubert *et al.*, The $e^+e^- \rightarrow 3(\pi^+\pi^-)$, $2(\pi^+\pi^-\pi^0)$ and $K^+K^-2(\pi^+\pi^-)$ cross sections at center-of-mass energies from production threshold to 4.5 GeV measured with initial-state radiation, Phys. Rev. D **73** (2006), 052003, https://doi.org/10.1103/PhysRevD.73.052003.

18. J. Lees *et al.* (BABAR Collaboration), Study of the process $e^+e^- \rightarrow \pi^+\pi^-\eta$ using initial state radiation, Phys. Rev. D **97** (2018), 052007, https://doi.org/10.1103/PhysRevD.97.052007.

19. V. Ivanov *et al.*, Study of the process $e^+e^- \rightarrow K^+K^-\eta$ with the CMD-3 detector at the VEPP-2000 collider, Phys. Lett. B **798** (2019), 134946, https://doi.org/10.1016/j.physletb.2019.134946.

20. F. E. Close, A. Donnachie, Yu. S. Kalashnikova, Radiative decays of excited vector mesons, Phys. Rev. D **65** (2002) 092003, https://doi.org/10.1103/PhysRevD.65.092003.

21. M. N. Achasov *et al.* (SND collaboration), https://arxiv.org/abs/2110.05845.

22. T. Junk, Confidence level computation for combining searches with small statistics, Nucl. Instrum. Meth. A **434** (1999), 435, https://doi.org/10.1016/S0168-9002(99)00498-2.

23. A. L. Read, Presentation of search results: the CL_s technique, J. Phys. G **28** (2002), 2693, https://doi.org/10.1088/0954-3899/28/10/313.

24. M. N. Achasov *et al.*, Time resolution of the SND electromagnetic calorimeter, JINST **10** (2015), T06002, https://doi.org/10.1088/1748-0221/10/06/T06002.

25. M. N. Achasov *et al.*, Study of the process $e^+e^- \rightarrow n\bar{b}$ at the VEPP-2000 e^+e^- collider with the SND detector, Phys. Rev. D **90** (2014), 112007, https://doi.org/10.1103/PhysRevD.90.112007doi:10.1103/PhysRevD.90.112007, https://arxiv.org/abs/1410.3188.

26. V. M. Aulchenko *et al.*, The process $e^+e^- \rightarrow \omega\pi^0$ near the Φ resonance, J. Exp. Theor. Phys. **90** (2000), 927, https://doi.org/10.1134/1.559181.

27. M. N. Achasov *et al.*, Analysis of $e^+e^- \rightarrow \pi^+\pi^-\pi^+\pi^-$ and $e^+e^- \rightarrow \pi^+\pi^-\pi^0\pi^0$ processes in the energy range of $\sqrt{s} = 0.98 - 1.38$ GeV in experiments with a spherical neutral detector, J. Exp. Theor. Phys. **96** (2003), 789, https://doi.org/10.1134/1.1581933.

28. M. N. Achasov *et al.*, Study of process $e^+e^- \rightarrow \pi^+\pi^-\pi^0\pi^0$ at energies $\sqrt{s} < 1$ GeV with the spherical neutral detector, J. Exp. Theor. Phys. **109** (2009), 379, https://doi.org/10.1134/S1063776109090039.

29. J. P. Lees *et al.* (BaBar Collaboration), Measurement of the $e^+e^- \rightarrow \pi^+\pi^-\pi^0\pi^0$ cross section using initial-state radiation at BABAR, Phys. Rev. D **96** (2017), 092009, https://doi.org/10.1103/PhysRevD.96.092009.